

On the Nature of the B4 Banana Phase: Crystal or Not a Crystal?

David M. Walba,* Lior Eshdat, Eva Körblova, and Richard K. Shoemaker

University of Colorado, Department of Chemistry and Biochemistry,
215 UCB, Boulder, Colorado 80309-0215

Received June 19, 2005; Revised Manuscript Received August 19, 2005

ABSTRACT: Bent-core or banana-shaped liquid crystal mesogens are known to form chiral smectic phases from achiral or racemic molecules, representing the first example of conglomerate formation in bulk fluids. The most well studied examples of this behavior occur in the SmCP phases, subphases possessing the B2 chiral layer structure. However, the first description of chirality in the banana phase space was of the B4 phase, whose detailed structure is still under investigation. Indeed, the B4 phase is quite unique, and a consensus regarding the question of whether this phase is crystalline or liquid crystalline has not been reached. Here we describe data showing distinct differences, by NMR, between the SmCP phase and B4 phase of the prototypical banana phase mesogen **NOBOW** and, based upon an analysis of these data, suggest that the B4 phase is an unusual type of crystalline solid.

Introduction and Background

Organic crystal conglomerate formation, first observed by Pasteur in the most famous experiment in the history of organic stereochemistry,¹ continues to be of high current interest. As this report appears in a special issue of *Crystal Growth & Design* honoring Professor J. Michael McBride, it is worth pointing out that Professor McBride himself has published on solid conglomerates.²

Recently, work on the phenomenon of spontaneous reflection symmetry breaking in supermolecular ensembles has moved into fluid phases. To our knowledge, the first observation of conglomerate formation in a bulk fluid thermodynamic phase occurred for smectic liquid crystals (LCs), in the context of the study of “banana phases,” LC phases formed by bent-core mesogens.^{3–5} Specifically, as illustrated in Figure 1, the high-temperature LC phase of **NOBOW** (1; benzoic acid, 4-[[*E*]-[4-(nonyloxy)phenyl]imino]methyl]-, 1,3-phenylene ester), denoted B2,⁶ was observed in thin transparent capacitor cells to be composed of two coexisting antiferroelectric subphases: Sm_CA_PA and Sm_CS_PA. One of these, the Sm_CA_PA phase, was shown to exist as a conglomerate of chiral fluid domains.⁷

NOBOW is prototypical of a large class of banana phase mesogens with the B2–B3–B4 phase sequence [although in **NOBOW** the B3 phase is monotropic (metastable) and may not occur in bulk samples]. Early X-ray diffraction studies on such materials showed that the B2 phase (now understood to include four diastereomeric subphases;^{5,7} Figure 1C gives the structure of two of these diastereomers) is a fluid smectic LC, showing a sharp peak at a small angle deriving from the smectic layers and only a very diffuse peak at a wide angle, resulting from intermolecular spacings within the fluid layers. This X-ray signature is the same as that observed for a conventional calamitic (i.e., composed of rod-shaped mesogens) smectic A phase.

The B2 phase was an early target of intense investigation because the SmCP subphases are antiferroelec-

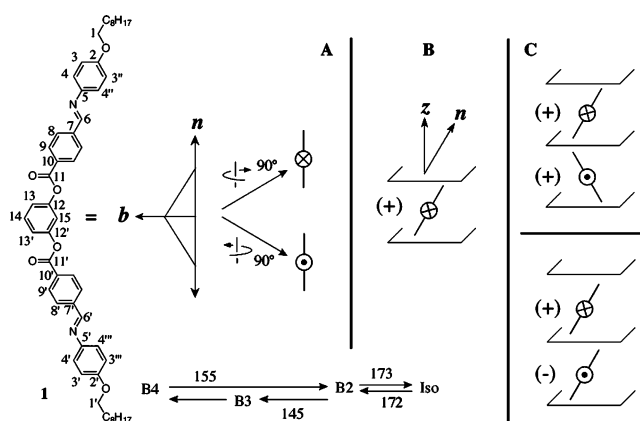


Figure 1. (A) The molecular structure of **NOBOW** (1) is given, with the carbon atom numbering scheme used in the text and the phase sequence and transition temperatures (°C) observed by polarized light microscopy in thin LC cells. (B) A schematic illustration of the B2 layer structure with positive chirality. (C) A schematic illustration of the structure of the two antiferroelectric B2 subphases: the Sm_CA_PA (polar smectic C, anticlinic, and antiferroelectric – top) and the Sm_CS_PA (synclitic and antiferroelectric – bottom).

tric or ferroelectric and exhibit (anti)ferroelectric electrooptics (EO); behavior previously seen only in LC phases composed of enantiomerically enriched mesogens.⁸ To illustrate the B2 layer structure, a bow and arrow analogy is useful for describing the geometry of the mesogens. As shown in Figure 1A, the molecular director (**n**), the average long axis of the molecules, is along the bowstring, while the **b**-vector is along the arrow. Projections of this construction with the arrow pointing back (⊗) and out (circled dot) are shown. Within a single B2 layer, **n** is tilted from the layer normal (**z**), and the **b**-vectors are parallel within layers, normal to the plane containing **z** and **n** (the tilt plane), as indicated in Figure 1B. The B2 phases are smectics, meaning that within each layer the structure is completely fluid (there is no long-range positional order within the layers). The B2 layers are chiral; positive

* To whom correspondence should be addressed. E-mail: walba@colorado.edu.

layers have **b** parallel to $\mathbf{z} \times \mathbf{n}$, as indicated in Figure 1B, while in negative layers **b** is reflected through the tilt plane and oriented antiparallel to $\mathbf{z} \times \mathbf{n}$. The SmCP subphases result from different stackings of identical B2 layers, with a two-layer periodicity.

In the B2 subphases, there are three independent supermolecular stereogenic elements, which differ in the relative configuration of adjacent pairs of layers. In a phase of infinite layers, for all adjacent layer pairs, **n** may tilt in the same direction (syn-clinic: dihedral angle between tilt planes = 0°) or in opposite directions (anti-clinic: dihedral angle between tilt planes = 180°), **b** may be parallel (ferroelectric) or antiparallel (antiferroelectric), and the relative chirality may be homochiral or heterochiral. This leads to four polar tilted smectic (SmCP) diastereomeric phases; two conglomerates and two macroscopic racemates. The structures of the two antiferroelectric diastereomers are indicated in Figure 1C. In Figure 1C (top), the supermolecular structure of the anti-clinic antiferroelectric polar smectic C isomer (+)-SmC_AP_A (subscripts refer to anti-clinic and antiferroelectric, respectively) is illustrated. This phase is chiral and exists as a conglomerate of chiral domains. In Figure 1C (bottom), the syn-clinic antiferroelectric isomer SmC_SP_A is illustrated. This phase is achiral and exists as a macroscopic racemate. The achiral SmCP diastereomers are analogous to meso compounds, achiral structures composed of chiral parts.

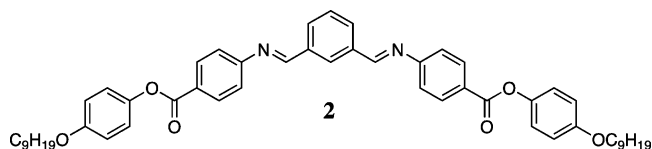
The antiferroelectric SmCP phases of **NOBOW** switch to corresponding ferroelectric states (without changing the chirality of the layers) upon application of an electric field, with a dramatic change in the observed texture by polarized light microscopy (PLM). This represents the first example of antiferroelectric behavior in a fluid phase composed of achiral molecules.³ The EO behavior of the SmC_AP_A phase is also the key to the elucidation of its chiral structure. The SmC_AP_A phase of **NOBOW** is obtained upon heating from the low-temperature B4 phase (see below). In samples of neat **NOBOW**, the chiral SmC_AP_A phase in transparent capacitor cells shows “conglomerate EO,” with heterochiral domains behaving in an enantiomeric fashion electrooptically.⁷ Doping the sample with a unichiral material can cause the collective free energy of one of the enantiomeric SmC_AP_A phases to be preferred such that only this enantiomer is formed in the cell, and “unichiral EO” is observed. The optic axis response and birefringence changes occurring upon switching of the enantiomeric antiferroelectric SmC_AP_A phases to the corresponding enantiomeric SmC_SP_F ferroelectric states provide the strongest evidence to date in support of the proposed chiral SmC_AP_A supermolecular structure shown in Figure 1C (top).

For a given material, the B3 phase always occurs at lower temperature than B2 (i.e., B3 has in general a lower collective entropy of formation than B2) and exhibits peaks by X-ray diffraction at wide angle, suggesting a hexatic structure. In hexatic smectic phases, there is no long-range positional order within layers, but there is long-range “bond orientational order”⁹ giving rise to X-ray diffraction peaks at wide angle. In this nomenclature, “bonds” simply represent the vector between the centers of neighboring molecules. In hexatic smectics, these vectors are oriented on a

hexagonal lattice with long-range order, even though the molecules have no long-range positional order within the layers.

The B4 Phase. The low-temperature B4 phase observed for the classic double Schiff's base bent-core materials such as **NOBOW** is highly unusual and has been studied extensively. This phase appears almost isotropic on micrometer length scales and has a complex supermolecular structure on the 10–500 nm length scale. The local structure and dynamics on the 10–100 Å length scale are not known. The B4 phase is not electrooptically active. However, this phase has properties suggesting it is chiral and exists as a conglomerate. Key experimental observations regarding the B4 phase are as follows.

Position in the Phase Sequence and Rheological Properties. In the earliest modern bent-core mesogen literature,¹⁰ the B4 phase was thought to be crystalline.³ To our knowledge, there has never been a reported example of a material possessing a liquid crystalline phase at lower temperature than B4 in the phase sequence. Many materials transition from a B3 phase into the B4 phase on cooling, the B4 then appearing stable at all lower temperatures. In relatively rare examples, a new crystalline phase appears below the B4 phase, with a relatively large enthalpy of formation.¹¹ For example, the **NOBOW** isomer **2** has the following phase sequence, transition temperatures (°C), and transition enthalpies on cooling (enthalpies in parentheses, kJ/mol) measured by differential scanning calorimetry: Cr – 132 (–45.8) – B4 – 145 (–37.2) – B2 – 149 (–12.0) – I.¹¹ From these data, it can be seen that the B4 phase is considerably more ordered (lower entropy of formation – at the transition, $\Delta G = 0$, and $\Delta H = T\Delta S$) than the smectic fluid B2 phase (transition entropy from B2 to B4 = –0.09 kJ/mol K) and also considerably less ordered than the low-temperature crystalline phase (transition entropy from B4 to crystal = –0.11 kJ/mol K). Thus, the loss of entropy at the B4–crystal transition is larger than that at the B2–B4 transition. This result is consistent with either a crystalline or a liquid crystalline B4 phase.



Some physical properties of the B4 phase, especially at high temperature, suggest the phase is liquid crystalline. In **NOBOW**, the transition into the B4 phase on cooling occurs at between 155 and 145 °C, depending upon the cooling rate and other details of the cell. At these high temperatures, qualitative rheological properties show the phase to be fluid. When present between a microscope slide and cover slip, the phase shears easily and takes the shape of its container. As the sample is cooled, the viscosity increases, until at room temperature and below, the phase behaves as a solid glass or crystal. No lower-temperature phase has been observed for **NOBOW**.

Polarized Light Microscopy (PLM). In thin cells between crossed polarizers, polarized visible light microscopy shows that the B4 phase is almost optically

isotropic, with only very weak birefringence in some preparations and somewhat higher birefringence in others. The B4 phase of **NOBOW** and the other classic B4 mesogens have a blue color by PLM in transmission, and the spectrum of reflected light has a sharp peak at 430 nm.¹² B4 in such cells can show relatively large ($> 100 \mu\text{m}^2$) domains with large uniform optical activity (rotations of plane polarized white light of $\sim 1^\circ/\mu\text{m}$ of sample). Domains of opposite handedness are easily identified by uncrossing the analyzer, and all domains have about the same magnitude of the optical activity.

Circular dichroism (CD), with the incident beam spot large relative to the domain size, is small and may be positive or negative depending upon the preparation. Doping of the sample with a unichiral mesogen biases the CD to one sign, without changing the wavelength of the peak in reflection. This behavior is consistent with a conglomerate of chiral domains.¹²

Another early report describes the behavior of "aligned" samples of the B4 phase.¹³ In "homogeneously aligned" B4 (in such cells, the director is supposed to be more or less parallel to the plane of the substrates), the blue reflection color for light incident normal to the substrate plane is seen, while in homeotropically aligned samples (director perpendicular to the substrates) the blue color was not seen. This led to the hypothesis that the B4 phase is a smectic possessing a helical periodicity, with the helix axis perpendicular to the director and parallel to the smectic layers, i.e., a twist grain boundary (TGB) phase.¹⁴ While it is difficult to reconcile the details of this experiment with more recent results, the proposal of a TGB-like structure of the B4 phase has held up remarkably well.

Finally, it has been reported that the chirality of domains in the B4 phase is maintained in the transition to the B2 phase.¹⁵ When a sample with a B2–B4 transition was cycled through the transition several times, the optically active domains became large, and it was seen that the shape of the domains, and their chirality, was conserved in the phase transition. While this behavior has not been shown for **NOBOW**, it is interesting to note that the achiral SmC_SP_A phase of **NOBOW** is apparently the thermodynamic phase, while melting into the B2 phase from the chiral B4 gives the chiral SmC_AP_A phase.⁷ Thus, the formation of the SmC_AP_A phase from B4 is under kinetic control. Apparently, there is also a kinetic preference for maintenance of the chirality of the B4 domains upon transition into the SmC_AP_A . While kinetic effects in LC phases are well-known (metastable "monotropic" LC phases often occur in supercooled crystalline materials), they are much less common in LC phases than in organic crystals. Typically, an LC phase observed upon heating from a lower temperature phase is assumed to be the thermodynamic global minimum of the system (an enantiotropic phase).

X-ray Diffraction. X-ray diffraction from bulk samples of B4 phase exhibit a strong smectic layer peak at small angle, and several broad peaks at wide angle.⁴ The small angle peak gives a layer spacing for the B4 phase substantially larger than that of the above-lying B2 phase. This result, combined with the apparent correlation between the chirality of the B4 and the SmC_AP_A phase, is especially interesting because if the

molecules in the B4 phase were indeed completely untilted, the basis of the chirality in the SmC_AP_A phase, the tilt of the director normal to the polar axis, would be lost.

The wide angle peaks observed for the B4 phase are broader than those originating from the hexatic in-layer order of the B3, suggesting that the B4 phase is somehow less ordered than B3. However, as mentioned above, the B4 phase always comes below the B3 in temperature. In materials where there is a B4–crystal transition, the wide angle peaks from the crystal phase are many and sharp, as expected for a crystalline structure. Taken together, these results regarding the wide-angle scattering seem a bit contradictory. However, high-resolution X-ray diffraction experiments illuminate the situation. Specifically, the peak width at half-maximum intensity for the small angle smectic layer peak of B4 is actually relatively large, suggesting a coherence length for the smectic layers of only about 200 Å.¹⁶ Thus, the observed broad peaks at wide angle is consistent with either locally crystalline order in small domains or liquid crystalline hexatic in-layer order in small domains, in B4.

Atomic Force Microscopy and Freeze Fracture Transmission Electron Microscopy. Early atomic force microscopy imaging studies on B4 samples frozen into the solid or glass phase corroborate the TGB-like structural hypothesis.¹⁷ Recently, several high-temperature phases with some apparent similarities to the B4 phase have been described. The "smectic blue" phases, which occur in chiral calamitic smectics,¹⁸ and the high-temperature dark conglomerate phase in bananas (the B4 phase is also one of the "dark conglomerates," meaning a conglomerate of optically active domains with low birefringence – dark between crossed polarizers), seem to involve defect lattices stabilized by a preference for saddle splay (negative Gaussian curvature) of the layers. Kamien has suggested a detailed model for the layer structure of the smectic blue phases dominated by saddle splay,¹⁹ while Clark has obtained data using freeze fracture transmission electron microscopy on the high-temperature dark conglomerate phases suggesting a structure similar to the lyotropic sponge phase or L_3 phase,²⁰ again dominated by saddle splay.²¹ It has been proposed that the high-temperature dark conglomerate is a kind of disordered smectic blue structure but with spontaneous reflection symmetry breaking.²¹ It is important to note that the high-temperature dark conglomerates and smectic blue phases always occur at the top of the LC temperature range, just below the isotropic; the defect lattice increases the entropy of the system relative to a normal smectic phase. The same phenomenon is well-known for the nematic blue phases, consisting of defect lattices of double twist tubes,²² which always occur above the normal nematic phase in temperature.

Dielectric Spectroscopy. A fairly detailed study of the dielectric response in the B2 and B4 phases of compound **2** in the frequency range from 0.1 to 10 MHz has been described.¹¹ This study, while provocative, proved to be inconclusive. A definitive interpretation of the dielectric response of either the B2 or the B4 phase in the context of a model for the structure of the phases was not possible. It is noted by these authors, however,

that the B4 phase does not behave as expected for a “classical solid modification.”

Second Harmonic Generation (SHG). The B4 phase has been reported to be SHG active, which limits the possible symmetries of the phase on a length scale on the order of microns.²³ Consistent with the apparent relationship between B4 and the polar (C_2) SmC_{AP_A} phase, this result shows that B4 cannot possess the D_2 symmetry of one of the antiferroelectric B2 phases, including the apparently closely related **NOBOW** SmC_{AP_A} phase, which is not SHG active.

NMR. Some of the earliest reported experiments in the banana phase literature involved cross-polarization/magic angle spinning (CP/MAS) ^{13}C NMR investigations of the B2 and B4 phases. Pelzl et al. reported results for the B2 phase of a symmetrical banana, which were consistent with the $SmCP$ proposal. However, in a series of influential papers, Watanabe et al. reported a remarkable “splitting” of the carbonyl peak into two peaks of approximately equal intensity in the B2 phase of the di-octyloxy homologue of **NOBOW**, **P-8-O-PIMB**.¹² This doubling was also observed in the B4 phase. In a careful reinvestigation of the ^{13}C NMR behavior of the system, this time using the di-tetradecyloxy-homologue of **NOBOW** (**P-14-O-PIMB**), it was reported that the B2 and B4 phases were not distinguishable by CP/MAS ^{13}C NMR,²⁴ with both phases showing the doubling of the carbonyl carbon peak. It was also reported in this work that the $SmC_S P_A$ and SmC_{AP_A} phases give the same spectrum. In this experiment, the SmC_{AP_A} phase was presumably obtained by cycling between the B4 and B2 phases in the spectrometer, then holding in the B2 temperature range.

From the beginning of the banana phase story, the observed doubling of the carbonyl peak in the CP/MAS spectrum of the B2 phase has been the focus of intense speculation. Watanabe et al. took this result as an indication that, in the smectic phase, the conformational motions of the phenylbenzoate units in the bent-core structure was “frozen” on the NMR time scale. Many calculations, culminating in a high-quality study of the conformational surface of 1,3-benzenediol dibenzoate using density functional theory,²⁵ show that these conformations are chiral, which led to the very widely discussed “conformational chirality” proposal occurring in smectic LCs.^{12,13,26} According to this proposal, the chirality of the phenylbenzoate conformations in the banana structure are at least partly responsible for the spontaneous reflection symmetry breaking, which occurs in the B2 layer structure.

The calculations all suggest a low barrier for interconversion between enantiomeric conformations in the gas phase. The conformational chirality hypothesis requires that in the smectic phase these conformations are “frozen” by intermolecular interactions in the smectic LC local environment. While this phenomenon is well-known in crystalline solids, to our knowledge it had not been considered relevant in LCs until the banana phase conglomerates were discovered.

The concept of conformational chirality in LCs has led to a search for other novel chirality phenomena in the bent core system in addition to the formation of chiral B2 layers. Some highlights include: (1) a hypothesized helical supermolecular structure in the B2 and

B4 phases of **P-8-O-PIMB**;^{12,13} (2) the observation that doping of an “achiral” banana phase mesogen into a chiral nematic phase *tightens* the helical pitch of the phase;²⁷ and (3) formation of a chiral nematic phase from an achiral bent-core mesogen.²⁸ Recently, this search for novel examples of reflection symmetry breaking has extended to calamitic systems. Spontaneous deracemization in a racemic chiral smectic has been reported;²⁹ and finally, evidence for the formation of a chiral SmC phase of the classic calamitic achiral smectic mesogen p,p'-di-octyloxy phenylbenzoate has been described.³⁰

It is suggested here, without proof or discussion, that simpler alternative explanations exist for the observations leading to all of the above suggestions of reflection symmetry breaking in fluids. In this context, it seems valuable to point out that in LC cells, an achiral phase can easily give rise to a chiral director structure and show properties such as optical activity and CD. In fact, this was first demonstrated by Mauguin and reported in his famous 1911 paper describing an optically active twisted nematic structure between mica substrates, from an achiral LC.³¹ The origin of the chirality in this case is driven by surface constraints, and this work proved to be a key foundation of the LC display industry, which began more than 50 years later. Also, the CD signals obtained from twisted nematic cells have been analyzed in detail.³² Finally, conglomerate electrooptics can be seen in LC cells containing achiral LC phases. For example, in nematic droplets surrounded by isotropic liquid, a complex twisted nematic structure, enforced by the interfaces, can provide chiral electrooptics³³ due to the flexoelectric effect.³⁴

With regard specifically to the banana phases, the original hypothesis of a helical structure in the B2 phase^{12,13} was based upon EO observations in LC cells. The reported EO behavior is now known to be diagnostic of the $SmC_S P_A$ phase, a macroscopic racemate.⁷ No evidence for a helical superstructure has been demonstrated for the $SmC_S P_A$ phase, which in fact shows achiral EO.

However, the “conformational chirality” hypothesis has become so widespread in the smectic LC literature that it seemed important to reexamine the classic B2 and B4 phases by NMR because NMR data was the original source of the hypothesis. In addition, the question of whether the B4 phase is crystalline or liquid crystalline seems especially interesting because if the B4 phase is an LC phase, the demonstration of its chirality would represent the first correct description of an LC conglomerate. Of course, if the B4 phase proves to be crystalline, it represents another in a long line of examples³⁵ of spontaneous reflection symmetry breaking in the formation of organic crystals leading back to Pasteur in the mid-nineteenth century,¹ albeit a very unique and interesting kind of crystalline phase.

Experimental Section

Samples of **NOBOW** were prepared according to Matsunaga.³⁶ ^{13}C magic angle spinning (MAS) NMR spectra were recorded on a Varian INOVA 400 spectrometer, with a Larmor frequency of 400 MHz for 1H and 100 MHz for ^{13}C . MAS spectra were obtained using a 4-mm narrow bore probe and a spinning rate = 10.5 kHz, with 1–2 K repetitions. Spectra

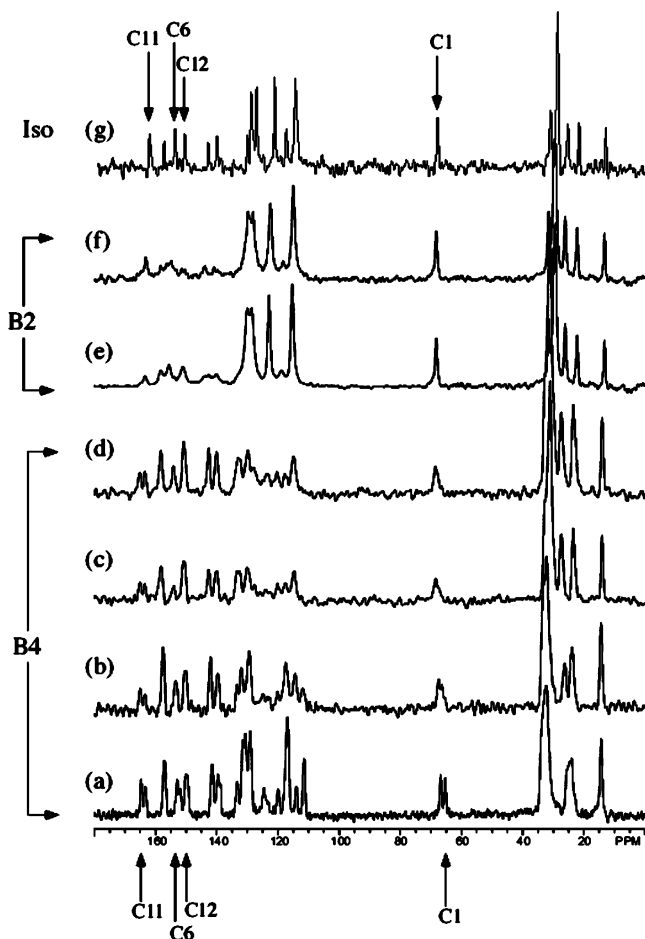


Figure 2. ^{13}C CP and single pulse MAS NMR of NOBOW at various temperatures. (a–d) CP/MAS of the B4 phase at 20, 85, 144, and 152 (on cooling from the B2 phase) $^{\circ}\text{C}$, respectively; (e) CP/MAS of the B2 phase at 158 $^{\circ}\text{C}$; (f) single-pulse MAS of the B2 phase at 158 $^{\circ}\text{C}$; (g) single-pulse ^{13}C spectrum of the isotropic phase at 181 $^{\circ}\text{C}$.

were recorded at variable calibrated temperatures³⁷ in the temperature range from 20 to 181 $^{\circ}\text{C}$.

Cross-polarization was carried out using a Hartmann–Hahn spin lock field corresponding to 72 kHz, while applying a linear ramp on the ^{13}C spin-lock power to ensure full polarization of all carbon species. High-power proton decoupling was carried out during ^{13}C data acquisition using a 74 kHz decoupling field and TPPM modulation. Two-dimensional (2-D) exchange spectroscopy (EXSY) was performed with cross-polarization and was acquired and processed in phase-sensitive mode. ^1H dipolar coupling measurements were performed under magic angle spinning conditions. Variable temperature ^1H MAS experiments were performed to estimate the magnitude of the homonuclear dipolar coupling. The spinning angle was adjusted precisely to the magic angle using the ^{79}Br resonance of KBr. Assignment of all carbon peaks in solution was performed using 2-D NMR techniques (g-COSY, g-ROESY, HMBC, and HSQC). Assignments of the ^{13}C peaks in the B2 and B4 phases were extrapolated from the solution spectra.

Results and Discussion

An overview of the observed ^{13}C CP/MAS spectra for NOBOW for the temperature range from 20 to 181 $^{\circ}\text{C}$, is given in Figure 2. At 20 $^{\circ}\text{C}$ (Figure 2a), the CP spectrum exhibits the expected aliphatic, alkoxy (C1), aromatic, Schiff's base (C6), and carbonyl (C11) signals. In addition to the doubling of the carbonyl carbon signal

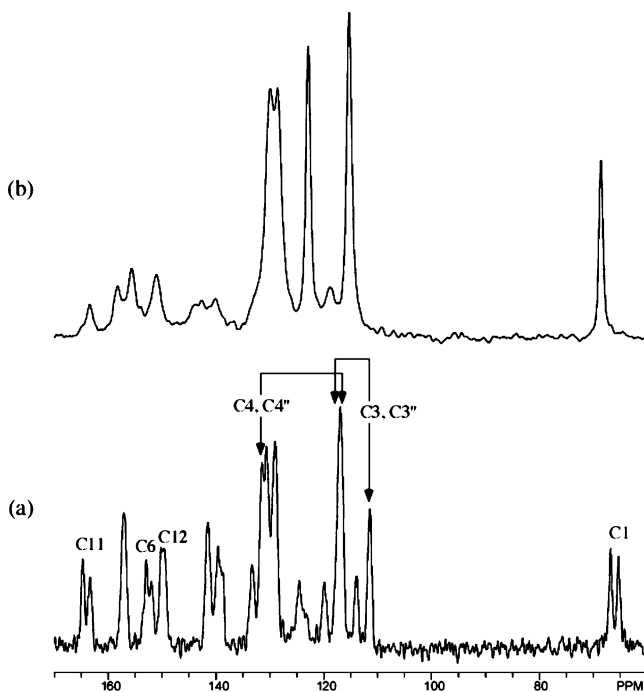


Figure 3. Expansions of the region from 60 to 170 ppm, showing the CP/MAS spectra of NOBOW taken at 20 $^{\circ}\text{C}$ in the B4 phase (a) and at 158 $^{\circ}\text{C}$ in the B2 phase (b).

previously reported for the B4 phase of P-8-O-PIMB and P-14-O-PIMB,^{12,24} the CP spectrum reveals additional doubled peaks in the B4 phase for the alkoxy carbon (C1), C12, and C6 (the Schiff base carbon), as can be seen in Figure 3. In the spectra reported in ref 24, the alkoxy signal at room-temperature overlaps a spinning sideband. In the present study, the much higher spinning rate removes the sidebands, making it clear that the alkoxy signal is doubled.

To investigate the possibility of slow chemical exchange between the two peaks observed for the alkoxy carbon (C1) and the carbonyl carbon (C11), a 2-D EXSY³⁸ experiment was performed, using cross-polarization, at several temperatures in the B4 temperature range. As shown in Figure 4, no exchange cross-peak signal between the C1 and C1' or between C11 and C11' is observed, even when using a mixing time of 2 s at 151 $^{\circ}\text{C}$ (close to the upper limit of the B4 temperature range). Thus, within our ability to measure exchange, there appears to be no interconversion of the two peaks from the carbonyl (C11) carbon or the alkoxy (C1) carbon on the time scale of 1–2 s. Importantly, it is also clear, as can be seen in Figure 4, that C3 and C4 carbons are split in the B4 phase due to a slow phenyl ring rotation. This splitting is also indicated in Figure 3. Analysis of the EXSY data suggests a rotation rate of the terminal aromatic rings on the order of 0.5 Hz ($\Delta G^{\ddagger} = 17.3\text{--}17.7 \pm 0.2 \text{ Kcal mol}^{-1}$), in the B4 phase at 20 $^{\circ}\text{C}$. Given that similar dynamics have been observed in conventional organic crystals,³⁹ this result is consistent with a locally crystalline structure and difficult to rationalize for a locally fluid structure.

Interestingly, the downfield part in each pair of the doubled signals has a slightly stronger intensity when the sample is heated (Figure 2a–c). But they are closely equivalent when the sample is cooled from the B2 phase (Figure 2d).

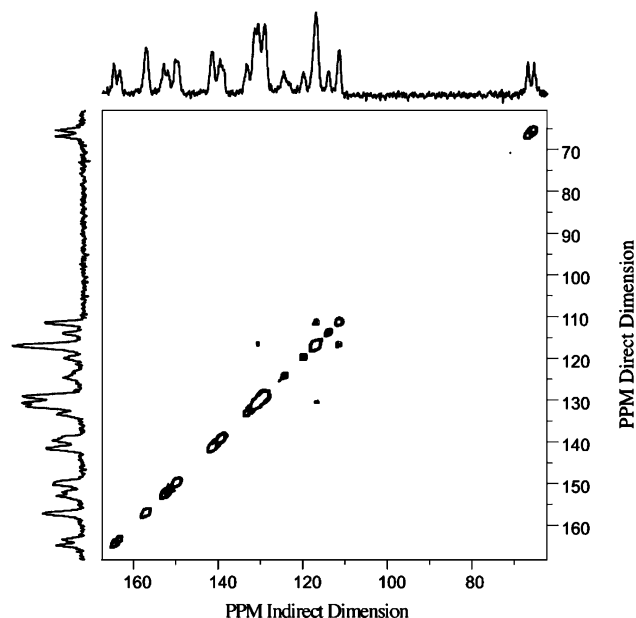


Figure 4. 2-D exchange spectroscopy (EXSY) spectra of the B4 phase at 20 °C, using a mixing time of 1.0 s.

At higher temperatures in the B4 phase (Figure 2b–d), the spectra reveal a temperature-dependent change in the chemical shift of the alkoxy (C1) signals (and of a few aromatic and aliphatic signals as well), which converge at the highest temperature of the B4 phase range (Figure 2d). A similar convergence of chemical shift occurs for the splittings of C3 and C4.

Heating the sample to 3 °C above the B4–B2 transition (158 °C) yields a new spectrum attributed to the B2 phase (Figure 2e,f). Although the chemical shifts of the carbon peaks change very little, there are dramatic differences between the spectrum from the B4 phase and that from B2 phase: (1) No doubling of carbon signals can be seen in the B2 phase; and (2) The nonprotonated carbon signals are much weaker in the B2 spectrum relative to signals from carbons directly bonded to protons. In the CP/MAS spectrum of the B4 phase, all of the carbon peaks are fully cross-polarized.

These observations in the B2 temperature range are fully consistent with a fluid smectic SmC_AP_A or SmC_SP_A liquid crystalline structure. The homotopic nature of C11 and C11' on the NMR time scale is fully expected for a smectic LC, as is true for C1, C6, and C12 as well. The low intensity of the signals for nonprotonated carbons is also expected for a smectic LC because the reduction in the homonuclear, intermolecular dipolar coupling occurring in a fluid due to cross-polarization behavior is that of an isolated ^1H - ^{13}C spin system. Protonated carbons undergo cross-polarization rapidly, but carbon nuclei that are not directly bonded to protons show very weak cross polarization.⁴⁰ In fact, a spectrum of the B2 phase could be acquired by using the single-pulse sequence, due to fast relaxation in the smectic LC. The spectrum obtained from the B4 phase in a single-pulse experiment at 152 °C shows relatively sharp aliphatic signals but very broad aromatic signals due to long relaxation constants for the latter and short ones for the former. This is consistent with a local structure where the cores are much less conformationally mobile than the tails in the B4 phase.

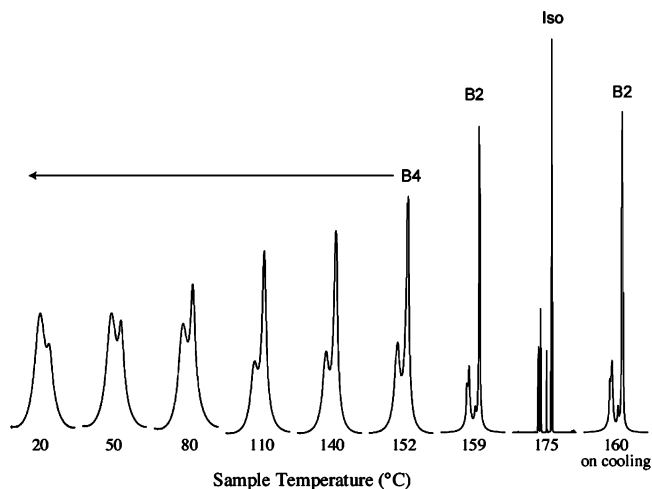


Figure 5. Single pulse variable temperature ^1H MAS NMR spectra of NOBOW in the B2, B4, and isotropic phases. The displayed region for each spectrum ranges from 20 ppm to -10 ppm vs TMS.

Above the transition into the isotropic phase, no ^{13}C signal from cross-polarization is observable, and ^{13}C NMR observation is only possible using single-pulse direct excitation of ^{13}C (Figure 2g). Upon cooling of the sample back to the B2 phase, the ^{13}C spectra (both CP/MAS, and single pulse MAS) are essentially the same as those observed upon heating from the B4 phase. Thus, if the global minimum SmC_SP_A phase is formed on cooling from the isotropic phase, and the kinetically favored SmC_AP_A phase is formed upon heating from the B4 phase, then the SmC_AP_A and SmC_SP_A phases are indistinguishable by these NMR probes. Alternatively, it is possible that the SmC_AP_A phase observed in thin cells is actually stabilized by the surfaces and that in the bulk this phase is not observed. It should be pointed out that only one, resolution-limited smectic layer peak has ever been observed for NOBOW in bulk samples by small-angle X-ray scattering, even when the experiments were designed specifically to probe for coexistence of the two SmCP phases clearly present in thin cells.⁴¹ All attempts to observe an NMR spectrum for the monotropic B3 phase upon further cooling simply gave a spectrum similar to that of the B4 phase.

To further investigate the nature of the B4 phase, VT ^1H MAS single-pulse measurements and qualitative relaxation measurements were performed. The VT ^1H MAS NMR spectra presented in Figure 5 show homogeneous broadening in the B4 phase at room temperature, which is indicative of a crystalline solid or frozen glass. As the temperature is increased, there is a narrowing of signals from the aliphatic protons, indicating increased motion in the aliphatic side-chains; however, the spinning-sidebands still appear as a homogeneously broadened (strongly dipolar coupled) proton spin system with a dipolar coupling ($\Delta\omega_{\text{dipolar}}$) of ~ 40 kHz. At the highest temperatures in the B4 range, the overall dipolar coupling is ~ 22 kHz. In the B2 phase, $\Delta\omega_{\text{dipolar}}$ drops to much less than 10 kHz, and the spectrum gives the appearance of a heterogeneously broadened line (see Supporting Information for the spectrum showing spinning sidebands and details on the derivation of $\Delta\omega_{\text{dipolar}}$). This is consistent with the liquidlike motion in the

smectic layers greatly attenuating intermolecular dipolar coupling in the B2 phase.

Qualitative relaxation constant measurements support the picture suggested by the VT ^1H MAS NMR results. The overall $T_1(\rho)$ for carbons decreases upon heating from room temperature to 152 °C and then increases to 6.6 ms at 158 °C. This is in accordance with a solid that has significant motion (spectral density) at or near 72 kHz (our spin-locking field). The increase in $T_1(\rho)$ in the B2 phase can be explained by divergence from 72 kHz due to high molecular motion.

At room temperature, the aromatic carbons have a $T_1 > 40$ s, while the aliphatic carbons have a T_1 around 3–5 s. At higher temperatures, the aliphatic carbon relaxation decreases slightly but not significantly. In the B2 phase, the T_1 of the protonated aromatic carbons drops to < 2 s, actually slightly less than the aliphatic carbons. Overall, the carbon T_1 relaxation time constants are all less than 3 s in the B2 phase, as observed by direct (single pulse) carbon experiments.

Conclusions

The results presented here show an easily observed B4–B2 phase transition by ^{13}C CP/MAS NMR spectroscopy. The data taken in the B2 temperature range suggest a fluid smectic, fully consistent with the proposed SmCP structure.⁷ If there is coexistence between the SmC₅P_A ground state and a metastable SmC_AP_A phase, this cannot be seen in these experiments. Either there is no coexistence in the bulk samples or the two SmCP phases show indistinguishable NMR spectra under these conditions.

The previously observed “splitting” or doubling of certain carbon peaks in the B2 phase^{12,15} is not seen in our experiments, which strongly suggests that prior data was actually obtained in the B4 phase not the B2 phase. Thus, the LC “conformational chirality” hypothesis, which explicitly states that interconversion between chiral phenylbenzoate conformations is slow on the NMR time scale in the B2 phase is inconsistent with the data presented here.

In contrast, the previously reported doubling of the carbonyl carbon peaks in the B4 phase is fully reproduced in this work, with additional doublings also observed. It is interesting that two, and only two, peaks can be seen for the carbon atoms in question. The intensity of the two peaks in each case is very close, but the data do not rule out the possibility that these diastereotopic atoms are present in unequal number density.

Possible explanations for the observed ^{13}C CP/MAS spectra in the B4 phase include the following. First, the B4 phase may be crystalline on the 200 Å length scale, and the symmetry of the molecules is C₁. In this case, the molecules would be chiral, with enantiomeric domains possessing enantiomeric conformations, which are persistent on a long time scale. The carbonyl carbons (C11 and C11'), as well as all of the other corresponding carbons in the “top” and “bottom” halves of the molecules (C1 – C13, and C1' – C13', respectively), would be diastereotopic, and could give rise to two peaks of equal intensity in the ^{13}C CP/MAS spectrum. This is the “conformational chirality” argument applied to a crystalline material and is not unusual. A second related

possibility is that in a locally crystalline B4 phase, symmetry exists such that the top and bottom halves of the molecules are homotopic, but the crystal structure possesses two diastereotopic molecules in the unit cell.

A very different scenario posits a novel liquid crystalline B4 phase. It is possible that a smectic, TGB-like structure could exhibit a persistent diastereotopic relationship between carbons in the top and bottom halves of the molecules, if the layer structure in the smectic LC has C₁ symmetry. This possibility has been discussed extensively in the banana phase literature in the context of the “general polar smectic” phase or SmCPG.^{4,42} In the SmCPG layer structure, there is a component of the **b**-vector oriented along the layer normal **z** (in the SmCP layer structure, **b** is parallel to the layers). For example, the bow string **n** could be tilted from **z**, and the molecules could be rotated about **n** by less than 90°, in their equilibrium orientation, such that **b** is not parallel to the layers nor in the tilt plane.

The B4 phase could represent a variant of a SmCPG phase with additional long-range in-layer order giving rise to the wide-angle peaks in the X-ray, such as a hexatic SmCPG phase. In a SmCPG-type B4 phase, there could be rapid equilibration between conformations, as expected for a fluid smectic, but the top and bottom halves of the molecules would be diastereotopic due to the polar symmetry along **z**, giving rise to the observed doubling of carbon peaks. This is a fascinating possibility. But while a vigorous search for phases with a SmCPG layer structure is ongoing, to date no definitive evidence for the existence of a bulk SmCPG LC has been presented.

The hexatic TGB SmCPG proposal for the B4 phase is certainly highly exotic and attractive. However, taking into consideration the NMR results presented here (in particular, the slow rotation of the terminal phenyl rings of 0.5 Hz), the local structure on the length scale of the layer correlation length (~ 200 Å) of the B4 phase seems best described as follows. At low temperatures the B4 phase has a locally crystalline lattice of cores, with aliphatic tails that are frozen into a glassy state. At the high end of the B4 temperature range, the phase behaves as a locally crystalline lattice of cores, with the aliphatic tails far from the cores essentially melted into isotropic sublayers. The transition to the B2 phase is accompanied by the melting of the aromatic cores, giving a fluid SmCP phase.

The fluidlike rheological properties of the bulk B4 phase at high temperatures, and its unusual X-ray, dielectric, probe microscopy, and freeze-fracture TEM behavior, are all seemingly consistent with a “crystallized” TGB-like defect lattice stabilized by saddle splay. While the molecular origins of the tendency to give layers with negative Gaussian curvature are not known, local intermolecular interactions leading to twist on the length scale of several molecules could certainly be important. Apparently, in the B4 phase the preferred local structure cannot uniformly fill space, and a very dense defect lattice results. A less complex small length-scale defect lattice has been described for the modulated SmC₅P_F phase.⁴³ In this thermodynamic phase, the layers undulate sinusoidally, with a temperature-dependent period of about 20–50 nm, corresponding to the

width of stripes of splayed polarization. The origins of the splay stripes is likely steric.

Such defect-lattice LC structures are well-known and possess higher entropy than the corresponding conventional phases (nematic blue phase vs cholesteric, smectic blue phase vs SmA or SmC). This, plus the disorder in the tails in the frozen B4 at low temperature, seems a reasonable explanation for the considerably higher entropy of the B4 phase relative to a lower-lying crystal phase in materials possessing the Cr–B4 phase transition.

The formation of chiral crystal structures from achiral molecules is not unusual, and conformational chirality is often observed in crystals. With regard to the origins of the chirality of the B2 smectic LC layer structure, symmetry dictates that conformations, which are enantiomeric in the isotropic phase, must be diastereomeric in the SmCP layers, and therefore possess differing free energies. In a sense, there must be long-range “orientational order” of chiral conformations occurring in the SmCP layers. The key point of the “conformational chirality” hypothesis in the context of banana phases, however, is a freezing out of interconversion between enantiomeric conformations, such that they give rise to independent signals in the ^{13}C CP/MAS NMR spectrum and drive the formation of macroscopically chiral layers.

In our picture of the B2 phase, all chiral conformations are in rapid, dynamic equilibrium, as is true in the isotropic fluid. In the chiral B2 layers, enantiomeric conformations must be present in different number densities (which difference could be large or could be too small to observe) but are still in rapid equilibrium in the fluid smectic phases. Our basic hypothesis regarding the origins of the B2 chiral layer structure^{5,7} remains unchanged: This chiral structure is driven by a combination of spontaneous breaking of nonpolar symmetry, and by tilt of the director from the layer normal, both occurring due to steric, or space-filling considerations, which become dominant as entropy comes out of the system at the isotropic \rightarrow LC transition. The uniqueness of the B2 phases stems from the nonpolar symmetry breaking, and the steric argument for this aspect of the phase structure was considered important from the initial discovery of the electrooptically active banana phases.³ The chirality of conformations of the mesogens is not specifically relevant to the formation of the chiral layer structure in the B2 phases.

Acknowledgment. We thank the Liquid Crystal Materials Research Center (NSF MRSEC award no. DMR-0213918) for financial support of this work. The authors thank Professor Noel A. Clark and Dr. Michi Nakata for helpful discussions.

Supporting Information Available: Details on the derivation of $\Delta\omega_{\text{dipolar}}$, including variable-frequency, ^1H MAS NMR of B4 at 20 °C, and broad range VT ^1H MAS single pulse spectra showing the spinning sidebands. This material is available free of charge via the Internet at <http://pubs.acs.org>.

References

- Pasteur, L. *C. R. Acad. Sci.* **1848**, *26*, 535–539.
- McBride, J. M.; Carter, R. L. *Angew. Chem., Int. Ed. Engl.* **1991**, *30*, 293–295.
- Niori, T.; Sekine, T.; Watanabe, J.; Furukawa, T.; Takezoe, H. *J. Mater. Chem.* **1996**, *6*, 1231–1233.
- Pelzl, G.; Diele, S.; Weissflog, W. *Adv. Mater.* **1999**, *11*, 707–724.
- Walba, D. M., *Ferroelectric liquid crystal conglomerates*. In *Topics in Stereochemistry, Materials-Chirality*; Green, M. M.; Nolte, R. J. M.; Meijer, E. W.; Denmark, S. E., Eds.; Wiley: New York, 2003; Vol. 24, pp 457–518.
- The “B-phase” nomenclature was established in 1997 during the workshop “On Banana Liquid Crystals – Chirality by Achiral Molecules,” hosted by G. Heppke, December 10–11, 1997, Berlin. See <http://www.tu-berlin.de/~insi/ag_heppke/banana/materials.html>
- Link, D. R.; Natale, G.; Shao, R.; MacLennan, J. E.; Clark, N. A.; Körblová, E.; Walba, D. M. *Science* **1997**, *278*, 1924–1927.
- (a) Clark, N. A.; Lagerwall, S. T. *Appl. Phys. Lett.* **1980**, *36*, 899–901. (b) Lagerwall, S. T. *Ferroelectric and Antiferroelectric Liquid Crystals*; Wiley-VCH: Weinheim, Germany, 1999; p 427. (c) Walba, D. M., *Ferroelectric Liquid Crystals: A Unique State of Matter*. In *Advances in the Synthesis and Reactivity of Solids*; Mallouk, T. E., Ed. JAI Press Ltd: Greenwich, CT, 1991; Vol. 1, pp 173–235.
- Bruinsma, R.; Nelson, D. R. *Phys. Rev. B* **1981**, *23*, 402–410.
- Bent-core mesogens were first reported in the 1920s: (a) Vorländer, D.; Apel, A. *Ber. Dtsch. Chem. Ges.* **1929**, *62*, 2831. (b) Pelzl, G.; Wirth, I.; Weissflog, W. *Liq. Cryst.* **2001**, *28*, 969–972.
- Nadasi, H.; Lischka, C.; Weissflog, W.; Wirth, I.; Diele, S.; Pelzl, G.; Kresse, H. *Mol. Cryst. Liq. Cryst.* **2003**, *399*, 69–84.
- Sekine, T.; Niori, T.; Sone, M.; Watanabe, J.; Choi, S.-W.; Takamishi, Y.; Takezoe, H. *Jpn. J. Appl. Phys.* **1997**, *36*, 6455–6463.
- Sekine, T.; Niori, T.; Watanabe, J.; Furukawa, T.; Choi, S. W.; Takezoe, H. *J. Mater. Chem.* **1997**, *7*, 1307–1309.
- (a) de Gennes, P. G. *Solid State Commun.* **1972**, *10*, 753. (b) Renn, S. R.; Lubensky, T. C. *Phys. Rev. A* **1988**, *38*, 2132–2147.
- Niwano, H.; Nakata, M.; Thisayukta, J.; Link, D. R.; Takezoe, H.; Watanabe, J. *J. Phys. Chem. B* **2004**, *108*, 14889–14896.
- Results from Noel A. Clark, to be published.
- Heppke, G.; Moro, D. *Science* **1998**, *279*, 1872–1873.
- (a) Grelet, E.; Pansu, B.; Li, M. H.; Nguyen, H. T. *Phys. Rev. E* **2002**, *65*, 050701(R). (b) Grelet, E.; Pansu, B.; Li, M. H.; Nguyen, H. T. *Phys. Rev. Lett.* **2001**, *86*, 3791–3794.
- DiDonna, B. A.; Kamien, R. D. *Phys. Rev. Lett.* **2002**, *89*, 215504.
- (a) Porte, G.; Marignan, J.; Bassereau, P.; May, R. *J. Phys.* **1988**, *49*, 511–519. (b) Roux, D.; Cates, M. E.; Olsson, U.; Ball, R. C.; Nallet, F.; Belloq, A. M. *Europhys. Lett.* **1990**, *11*, 229–234.
- Hough, L. E.; Spannuth, M.; Jung, H. J.; Zasadzinski, J.; Krueker, D.; Heppke, G.; Walba, D.; Clark, N. *Bull. Am. Phys. Soc.* **2005**, *50*, 223.
- Crooker, P. P., *Blue Phases*. In *Chirality in Liquid Crystals*; Kitzerow, H. S.; Bahr, C., Eds.; Springer-Verlag: New York, 2001.
- (a) Macdonald, R.; Kentischer, F.; Warnick, P.; Heppke, G. *Phys. Rev. Lett.* **1998**, *81*, 4408–4411. (b) Choi, S. W.; Kinoshita, Y.; Park, B.; Takezoe, H.; Niori, T.; Watanabe, J. *Jpn. J. Appl. Phys. Part 1* **1998**, *37*, 3408–3411. (c) Kentischer, F.; Macdonald, R.; Warnick, P.; Heppke, G. *Liq. Cryst.* **1998**, *25*, 341–347.
- Kurosu, H.; Kawasaki, M.; Hirose, M.; Yamada, M.; Kang, S.; Thisayukta, J.; Sone, M.; Takezoe, H.; Watanabe, J. *J. Phys. Chem. A* **2004**, *108*, 4674–4678.
- Imase, T.; Kawachi, S.; Watanabe, J. *J. Mol. Struct.* **2001**, *560*, 275–281.
- Tschierske, C.; Dantlgraber, G. *Pramana-J. Phys.* **2003**, *61*, 455–481.
- Thisayukta, J.; Niwano, H.; Takezoe, H.; Watanabe, J. *J. Am. Chem. Soc.* **2002**, *124*, 3354–3358.
- Niori, T.; Yamamoto, J.; Yokoyama, H. *Mol. Cryst. Liq. Cryst.* **2004**, *409*, 475–482.
- Takanishi, Y.; Takezoe, H.; Suzuki, Y.; Kobayashi, I.; Yajima, T.; Terada, M.; Mikami, K. *Angew. Chem., Int. Ed.* **1999**, *38*, 2353–2356.

- (30) Kajitani, T.; Masu, H.; Kohmoto, S.; Yamamoto, M.; Yamaguchi, K.; Kishikawa, K. *J. Am. Chem. Soc.* **2005**, *127*, 1124–1125.
- (31) Mauguin, C. B. *Soc. Franc. Miner.* **1911**, *34*, 71.
- (32) Saeva, F. D.; Olin, G. R. *J. Am. Chem. Soc.* **1976**, *98*, 2709–2711.
- (33) Rudquist, P.; Körblova, E.; Walba, D. M.; Shao, R.; Clark, N. A.; MacLennan, J. E. *Liq. Cryst.* **1999**, *26*, 1555–1561.
- (34) Meyer, R. B. *Phys. Rev. Lett.* **1969**, *22*, 918.
- (35) Jacques, J.; Collet, A.; Wilen, S. H., *Enantiomers, Racemates, and Resolutions*; Krieger Publishing Company: Malabar, FL, 1994; p 447.
- (36) Akutagawa, T.; Matsunaga, Y.; Yasuhara, K. *Liq. Cryst.* **1994**, *17*, 659–666.
- (37) The large temperature difference between the temperature displayed by the instrument and the actual temperature of the sample was calibrated by using the ^{207}Pb chemical shift in lead nitrate as reference. See Takahashi, T., Kawashima, H., Sugisawa, H., Baba, T. *Solid State Nucl. Magn. Reson.* **1999**, *15*, 119–123.
- (38) (a) Hawkes, G. E.; Lian, L. Y.; Randall, E. W.; Sales K. D. *J. Magn. Reson.* **1985**, *65*, 173–177. (b) Perrin, C. L.; Dwyer, T. *J. Chem. Rev.* **1990**, *90*, 935–967. (c) Orell, K. G.; Sik, V. *Annu. Rep. NMR Spectrosc.* **1993**, *27*, 163–171.
- (39) (a) Harbison, G. S.; Raleigh, D. P.; Herzfeld, J.; Griffin, R. G. *J. Magn. Reson.* **1985**, *64*, 284–295. (b) Twyman, J. M.; Dobson, C. M. *Magn. Reson. Chem.* **1990**, *28*, 163–170.
- (40) Emsley, J. W. In *Solid-State NMR Spectroscopy Principles and Applications*; Duer, M. J. Ed.; Oxford, UK, 2002. Ch. 11.
- (41) Noel A. Clark, private communication.
- (42) (a) Brand, H. R.; Cladis, P. E.; Pleiner, H. *Eur. Phys. J. B* **1998**, *6*, 347–353. (b) Jakli, A.; Lischka, C.; Weissflog, W.; Pelzl, G. *Liq. Cryst.* **2000**, *27*, 715–719. (c) Jákli, A.; Krüerke, D.; Sawade, H.; Heppke, G. *Phys. Rev. Lett.* **2001**, *86*, 5715–5718. (d) Walba, D. M.; Korblova, E.; Shao, R.; Coleman, D. A.; Chattham, N.; MacLennan, J. E.; Clark, N. A. A General Polar Smectic C Banana Phase, International Liquid Crystals Conference 2002, Edinburgh, Scotland, June 30–July 5, 2002; Abstract, contributed lecture p C15. (e) Walba, D. M. In *The Smectic CPG Phases and NORABOW, Chirality and Polarity in the Liquid Crystal Banana Phases*, University of Colorado, Boulder, August 24, 2002; <http://anini.colorado.edu/bananas/walba.pdf>.
- (43) (a) Walba, D. M.; Körblova, E.; Shao, R.; MacLennan, J. E.; Link, D. R.; Glaser, M. A.; Clark, N. A. *Science* **2000**, *288*, 2181–2184. (b) Coleman, D. A.; Fernsler, J.; Chattham, N.; Nakata, M.; Takanishi, Y.; Korblova, E.; Link, D. R.; Shao, R. F.; Jang, W. G.; MacLennan, J. E.; Mondainn-Monval, O.; Boyer, C.; Weissflog, W.; Pelzl, G.; Chien, L. C.; Zasadzinski, J.; Watanabe, J.; Walba, D. M.; Takezoe, H.; Clark, N. A. *Science* **2003**, *301*, 1204–1211.

CG050282K